

TractGraphFormer: Anatomically Informed Hybrid Graph CNN-Transformer Network for Classification from Diffusion MRI Tractography

Yuqian Chen^a, Fan Zhang^b, Meng Wang^c, Leo R. Zekelman^d, Suheyla Cetin-Karayumak^e, Tengfei Xue^f, Chaoyi Zhang^f, Yang Song^g, Nikos Makris^h, Yogesh Rathi^e, Weidong Cai^f, Lauren J. O'Donnell^a

^a Department of Radiology, Brigham and Women's Hospital, Harvard Medical School, Boston, MA, USA

^b School of Information and Communication Engineering, University of Electronic Science and Technology of China, Chengdu, China

^c Beth Israel Deaconess Medical Center, Harvard Medical School, Boston, MA, USA

^d Department of Neurosurgery, Brigham and Women's Hospital, Harvard Medical School, Boston, MA, USA

^e Department of Psychiatry, Brigham and Women's Hospital, Harvard Medical School, Boston, MA, USA

^f School of Computer Science, The University of Sydney, Sydney, NSW, Australia

^g School of Computer Science and Engineering, University of New South Wales, Sydney, NSW, Australia

^h Departments of Psychiatry and Neurology, Massachusetts General Hospital, Harvard Medical School, Boston, MA, USA

Corresponding Authors: Fan Zhang (zhangfanmark@gmail.com) and Lauren J. O'Donnell (odonnell@bwh.harvard.edu)

Abstract

The relationship between brain connections and non-imaging phenotypes is increasingly studied using deep neural networks. However, the local and global properties of the brain's white matter networks are often overlooked in convolutional network design. We introduce TractGraphFormer, a hybrid Graph CNN-Transformer deep learning framework tailored for diffusion MRI tractography. This model leverages local anatomical characteristics and global feature dependencies of white matter structures. The Graph CNN module captures white matter geometry and grey matter connectivity to aggregate local features from anatomically similar white matter connections, while the Transformer module uses self-attention to enhance global information learning. Additionally, TractGraphFormer includes an attention module for interpreting predictive white matter connections. In sex prediction tests, TractGraphFormer shows strong performance in large datasets of children ($n=9345$) and young adults ($n=1065$). Overall, our approach suggests that widespread connections in the WM are predictive of the sex of an individual, and consistent predictive anatomical tracts are identified across the two datasets. The proposed approach highlights the potential of integrating local anatomical information and global feature dependencies to improve prediction performance in machine learning with diffusion MRI tractography.

Keywords: Sex classification, white matter tracts, Graph CNN, Transformer, dMRI tractography, deep learning

1 Introduction

The brain’s white matter (WM) connections (fiber tracts) and their tissue microstructure can be quantitatively mapped using diffusion magnetic resonance imaging (dMRI) tractography (Zhang et al., 2022b). The white matter fiber tract connections have important inter-individual variability, with implications for understanding neurodevelopment and disease (Forkel et al., 2022). Accordingly, one recent avenue of research explores white matter variability by predicting non-imaging phenotypes from dMRI tractography data using machine learning methods (Y. Chen et al., 2024; Gong et al., 2021; He et al., 2022; Xue et al., 2024). Non-imaging phenotypes can include demographic, behavioral, clinical and cognitive measures of subjects. These non-imaging phenotypes are predicted from input features describing the brain’s white matter connections, such as connectivity “strengths” or tissue microstructure measures (Zhang et al., 2022b).

The prediction tasks have been studied using traditional machine learning models such as Support Vector Machines (SVMs) (Feng et al., 2022; Zhang et al., 2018a), as well as deep methods such as convolutional neural networks (CNNs) (Chen et al., 2020; He et al., 2022; Jeong et al., 2021; W. Liu et al., 2023; Lo et al., 2024; Wei et al., 2023) or point-based neural networks (Chen et al., 2022; Y. Chen et al., 2024). For example, Feng et al. evaluated machine learning methods using multiple features describing WM connections for the prediction of individual performance across cognitive domains (Feng et al., 2022). In another example, (He et al., 2022) performed age and sex prediction using a CNN with input white matter microstructure and connectivity features extracted from dMRI tractography data.

However, challenges remain in the design of deep neural networks for prediction tasks based on white matter features. The brain’s white matter is organized into structural networks that have important local and global properties (Park and Friston, 2013). Thus we investigate two main deep network design challenges related to the local and global properties of WM features.

First, it is a challenge to leverage existing neuroanatomical knowledge about local neighborhoods of WM connections to guide neural network training. By guiding network convolutions to focus on neighborhoods of connections that have similar anatomy in the brain, we hypothesize that local feature learning and overall network performance can be enhanced. As illustrated in Fig. 1, similar WM connections can be defined as those with similar WM geometry (trajectory and location) or gray matter (GM) connectivity (connected GM regions). Though prediction tasks can potentially benefit from useful neuroanatomical information about the brain’s WM connections, off-the-shelf methods such as SVMs or CNNs generally ignore all anatomical information about the white matter connections.

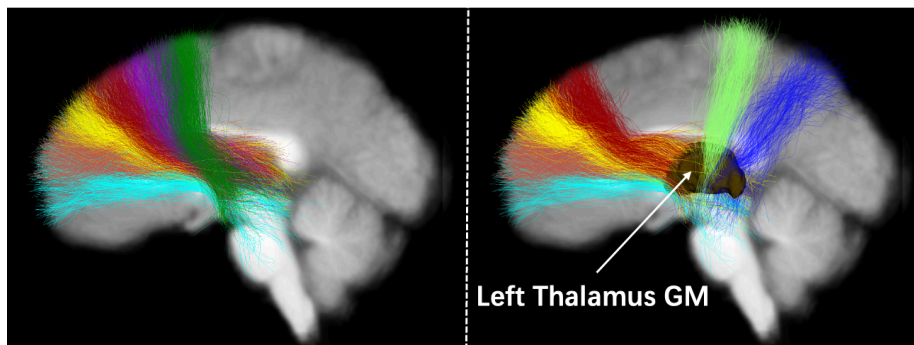


Fig. 1. Illustrations of WM connections with similar WM geometry (left) or GM connectivity (right). Each connection, or white matter fiber cluster, is shown in a unique color.

Second, it is a challenge for neural networks to capture global relationships between WM connections. Global information about WM features is expected to be important for tractography-related prediction tasks

because the human brain includes multiple interconnected structural networks that work together. We hypothesize that enhancing the learning of global information will improve network performance for tractography-based prediction. However, it is generally a challenge for off-the-shelf methods such as CNNs to fully capture global information (A. He et al., 2023).

To address the first challenge, a few studies have aimed to develop dedicated neural networks to utilize anatomical information for analyses of the brain’s structural connections. The BrainNETCNN (Kawahara et al., 2017) includes novel convolutional filters that improve performance (Yeung et al., 2020) by handling the topology of connectivity matrices (where each row or column corresponds to a gray matter (GM) region or node, and entries or edges in the matrix indicate connectivity strengths derived from the tractography connecting the GM regions). Other approaches apply graph convolutional neural networks to connectivity matrices, e.g., (Ktena et al., 2018). However, the above classes of methods are restricted to the anatomical information contained in the row and column structure of the connectivity matrix, and they cannot leverage any additional anatomical information to inform network convolutions.

To address the second challenge, a few studies have investigated the application of Transformers, which can learn global information and capture long-range interactions (A. He et al., 2023) in natural language processing (Vaswani et al., 2017) and computer vision tasks (Dosovitskiy et al., 2021). The initial applications of Transformers to tractography include one study that demonstrated benefits of learning global connectome patterns for the classification of Parkinson’s disease (Machado-Reyes et al., 2022). Another study (Zhang et al., 2022c) demonstrated the potential of transformers to identify discriminative tractography streamlines in the classification of schizophrenia. The advantages of transformers relate to their network structure. Comprising attention-driven building blocks, Transformers use a self-attention mechanism to model long-range interactions between all tokens (Vaswani et al., 2017). However, compared to CNNs, Transformers are weak in local feature learning and require larger training datasets.

Hybrid networks blending CNNs and Transformers have been proposed to leverage the strengths of each: CNNs for local feature learning and Transformers for global long-range dependency learning. These hybrids have found success in many computer vision applications (Wu et al., 2021; Zhang et al., 2023; Zheng et al., 2022). One related tractography analysis application has explored a hybrid network (Machado-Reyes et al., 2022) to successfully classify patients with Parkinson’s disease based on the structural connectome of the brain. This study proposed a basic Transformer architecture that leveraged a CNN for encoding the input connectomes. In our approach, we propose a hybrid CNN-Transformer network that is designed to specifically exploit the unique characteristics of white matter structures in dMRI tractography.

To focus our project, we choose a testbed problem of sex prediction. Sex is an important source of WM variability (Ingalhalikar et al., 2014), and WM has both local and global sex-related differences in its tissue microstructure (J. Chen et al., 2024). While sex prediction is not a straightforward problem, (Eikenes et al., 2022; Sanchis-Segura et al., 2022), several studies have demonstrated that features from quantitative dMRI tractography (Zhang et al., 2022b) are useful for sex classification (He et al., 2022; Kulkarni et al., 2013; Yeung et al., 2023, 2020). However, most existing methods have used a structural connectome matrix as input, which provides limited information about brain anatomy (Kulkarni et al., 2013; Yeung et al., 2023, 2020). In comparison with the traditional structural connectome matrix, fiber clusters enable consistent parcellation across the lifespan (Zhang et al., 2018c) with higher test-retest reproducibility (Zhang et al., 2019) and improve power to predict human traits (R. Liu et al., 2023). In addition, fiber clusters facilitate a compact vector representation of the connectome (R. Liu et al., 2023; Zhang et al., 2018a) and enable a variety of downstream statistical and machine learning analyses (Chen et al., 2023b; Gabusi et al., 2024; He et al., 2022; R. Liu et al., 2023; Xue et al., 2024; Zhang et al., 2018b). In this work, we leverage features from a white matter

tractography fiber cluster parcellation (Zhang et al., 2018c), which provides WM geometry and GM anatomical information for each cluster (Fig. 1) that we employ to enhance network design.

In this work, we propose a deep learning framework, TractGraphFormer, that focuses on local white matter anatomical neighborhoods while learning about global long-range feature dependencies among the brain’s connections. We design a hybrid two-stream neural network consisting of a Graph CNN and a Transformer module for sex prediction. The designed Graph CNN stream incorporates information about anatomical neighborhoods of WM connections to enhance performance of CNNs. The Transformer stream is integrated into the framework in parallel to the Graph CNN to establish long-range dependencies among clusters by self-attention, providing a supplement to the local convolution in the Graph CNN stream. A feature-level fusion strategy is employed to aggregate the local and global information learned by the Graph CNN and Transformer streams. In addition, an attention module is adopted to provide interpretability about the predictive WM tracts for sex classification. The main contributions of this paper are summarized as follows:

- We propose TractGraphFormer, a hybrid network consisting of Graph CNN and Transformer feature extractors for sex classification based on fiber cluster features.
- To learn anatomically informed local features, we model the anatomical relationship between clusters as a graph informed by WM geometry and/or GM connectivity. Then features from anatomically similar clusters are aggregated using a Graph CNN to improve performance.
- The Transformer stream is designed to extract global features and build long-range dependencies from all input clusters by naturally taking each cluster as a token.
- We propose to integrate a gated attention module into our framework to enable interpretation of predictive fiber clusters.
- We evaluate our method on two large-scale datasets of children and healthy young adults. The results show that the proposed method outperforms state-of-the-art methods in sex classification performance and identifies consistent predictive white matter connections across datasets.

The current paper extends a preliminary version of the work (Chen et al., 2023b) where we proposed the TractGraphCNN framework. In the current paper, we incorporate several technical improvements and additional analyses. First, based on the previous TractGraphCNN framework which extracts local features, we extend the network by adding a parallel Transformer module to extract global features and then fuse them to improve classification performance. We call the new proposed framework TractGraphFormer. Second, we propose a new combined graph that extends the two types of graphs in the preliminary work by simultaneously considering WM and GM information. We demonstrate the effectiveness of our method on the three types of graphs. Finally, we perform an extended set of experiments, including parameter tuning experiments to investigate classification performance under different parameter values and ablation studies to evaluate the effectiveness of our proposed modules. By incorporating these improvements, the paper strengthens the overall methodology and provides a more comprehensive evaluation of the proposed TractGraphFormer framework.

2 Methods

The overall workflow of the proposed method includes three steps. First, WM features are extracted from dMRI tractography fiber clusters (Section 2.1). Second, a graph is built to model the anatomical relationship between fiber clusters, informed by WM geometry and/or GM connectivity information (Section 2.2). Third, the built graph and WM features are input to the proposed TractGraphFormer framework (Section 2.3) for sex classification and interpretation of predictive tracts.

2.1 Study Dataset and Feature Extraction

In this study, we used two datasets of quantitative cluster-specific WM features. dMRI acquisitions were obtained from the Adolescent Brain Cognitive Development (ABCD) (Casey et al., 2018) and Human Connectome Project Young Adult (HCP-YA) (Van Essen et al., 2013) studies, and dMRI processing was performed as described below.

2.1.1 ABCD Dataset

To evaluate the performance of our proposed method, this study utilized dMRI data and demographic data (sex) of 9345 young children (47.8% female, 9.9 +/- 0.6 years old) from the large-scale, multi-site ABCD dataset (Casey et al., 2018). The dMRI data was originally acquired and minimally preprocessed by the ABCD study Data Analysis, Informatics, and Resource Center group ($b = 500, 1000, 2000$ and 3000 s/mm², resolution = $1.7 \times 1.7 \times 1.7$ mm³) (Zhang et al., 2022a). In this study, we used a derived database of harmonized and quality-controlled dMRI (Cetin-Karayumak et al., 2024) that was harmonized across 21 acquisition sites to remove scanner-specific biases while preserving inter-subject biological variability (Xue et al., 2024; Zhang et al., 2022a). For each subject, the dMRI data from the $b = 3000$ shell of all gradient directions and all $b = 0$ scans were extracted (Casey et al., 2018; Cetin-Karayumak et al., 2024). These data were used to perform tractography because this single shell can reduce computation time and memory usage while providing the highest angular resolution for tractography (Descoteaux et al., 2007; Ning et al., 2015; Zekelman et al., 2022).

2.1.2 HCP-YA Dataset

We also conducted experiments on the dMRI and demographic data (sex category) of 1065 healthy young adults (54.0% female, 28.7 +/- 3.7 years old) from the minimally preprocessed Human Connectome Project Young Adult (HCP-YA) dataset ($b = 1000, 2000$ and 3000 s/mm², TE/TR = 89/5520 ms, resolution = $1.25 \times 1.25 \times 1.25$ mm³) (Van Essen et al., 2013). For each subject, the dMRI data from the $b = 3000$ shell of all 90 gradient directions and all 18 $b = 0$ scans were extracted (Descoteaux et al., 2007; Ning et al., 2015; Zekelman et al., 2022).

2.1.3 White Matter Fiber Cluster Features

Whole brain tractography and white matter feature extraction were performed for the ABCD and HCP-YA datasets as follows (Cetin-Karayumak et al., 2024; Zekelman et al., 2022). First, whole brain tractography was obtained from the dMRI data using a two-tensor unscented Kalman filter tractography method (UKFt) (Reddy and Rathi, 2016) via SlicerDMRI (Norton et al., 2017; Zhang et al., 2020), as implemented in the ukftractography package¹. UKFt is highly consistent across the human lifespan, test-retest scans, disease states, and different acquisitions (Zhang et al., 2018c), and outperforms state-of-the-art tractography methods for reconstructing anatomical somatotopy (J. He et al., 2023). In contrast to other tractography methods that fit a model to the diffusion signal independently at each voxel, the UKFt framework employs prior information from the previous step during each tracking step to help stabilize model fitting (Zhang et al., 2018c). The two-tensor model adopted in the UKFt tractography algorithm can depict crossing streamlines, which are prevalent in white matter (Farquharson et al., 2013; Vos et al., 2013).

Second, tractography was parcellated using a machine learning approach that has been shown to consistently identify WM tracts across datasets, acquisitions, and the human lifespan (Zhang et al., 2018c), as implemented in the WMA package². This approach relies on an anatomically curated tractography atlas, the

¹ <https://github.com/pnlbwh/ukftractography>.

² <https://github.com/SlicerDMRI/whitematteranalysis>.

O’Donnell Research Group (ORG) Atlas (Zhang et al., 2018c). A description of the WM geometry and GM connectivity of each fiber cluster is provided in the ORG atlas, which includes 953 expert-curated fiber clusters categorized into 75 WM tracts. The ORG atlas enables automated exclusion of false positive streamlines. For each subject, parcellation produced 953 subject-specific fiber clusters. Importantly, cluster IDs were assigned according to the atlas and corresponded across subjects (e.g., cluster #1 corresponded across all subjects and datasets studied).

Finally, quantitative white matter features were computed for all clusters in both datasets. As previously described (Cetin-Karayumak et al., 2024; Zekelman et al., 2022), these computed WM features included fiber-specific microstructure measures computed from the multi-tensor model employed to perform tractography, including the mean fiber cluster fractional anisotropy (FA) and mean diffusivity (MD). These measures quantify the anisotropy and magnitude of water diffusion, providing indirect measures of the condition and geometry of the white matter tissue. These measures were computed following the typical practice of averaging across the microstructure values of all streamline points in the fiber cluster (Zhang et al., 2022b). Quantities related to the cluster geometry were also computed including the number of streamlines (NoS), which is a popular measure for the analysis of tractography (Zhang et al., 2022b). The above measures (FA, MD, and NoS) have previously been shown to be informative for the sex prediction task (J. Chen et al., 2024; Yeung et al., 2023, 2020). Since NoS is affected by intracranial volume, a common confound in sex prediction (Sanchis-Segura et al., 2022), in this work we propose to normalize NoS to reduce the effect of brain size by using the percentage of streamlines (PoS), which was calculated as the number of streamlines of a cluster divided by the total number of streamlines in all clusters of the subject. The input data for each subject (in ABCD and HCP-YA) was a cluster-wise WM feature matrix of size 3×953 . For absent clusters due to individual anatomical variation, we set features to zero (He et al., 2022; Xue et al., 2024). Finally, a min-max normalization was performed on the input feature matrix for FA, MD, and PoS individually.

2.2 Anatomically Informed Graph Construction

We propose to build graphs that model the anatomical relationship between fiber clusters. Each cluster is represented as a node in the proposed graph, with its cluster-specific WM features as node features. Edges are built to connect neighboring fiber clusters with similar anatomy. We propose three types of anatomically informed graphs, as described below.

2.2.1 Fiber Tract Geometry Informed Graph

The first type of graph (WMG) proposed in our study is based on WM tractography fiber geometric similarity, a well-established concept in the field of fiber clustering (Zhang et al., 2022b). The neighborhoods in WMG are defined according to fiber tract geometry. Specifically, we first compute the geometric distance between each pair of fiber clusters in the ORG atlas, which is measured as the mean of the pairwise fiber distances between the streamlines in the two fiber clusters. We use a popular fiber distance measure that has been used for over 20 years in the fiber clustering field, the mean closest point (computed using the minimum direct flip method) fiber distance (Garyfallidis et al., 2018; O’Donnell and Westin, 2007). A low distance between two clusters represents a high similarity in terms of WM anatomy. Then, for each cluster, we choose the top k clusters with the lowest geometric distances as neighbors, and edges are placed in between for graph construction.

2.2.2 Cortical and Subcortical Connectivity Informed Graph

The second type of graph (GMG) proposed in our study is based on GM regions to which the fiber clusters connect. The neighborhoods in GMG are defined according to connected GM regions of fiber clusters.

Specifically, for each cluster, we first identify its connected FreeSurfer (Fischl, 2012) GM regions. The ORG atlas provides the percentage of streamlines from each cluster that intersect each FreeSurfer region. We leverage this information to identify the top two FreeSurfer regions most commonly intersected by the streamlines of each cluster. The neighborhood of a cluster is then defined as the set of clusters with at least two top FreeSurfer regions in common, and edges are placed in between for graph construction.

2.2.3 Combined WM and GM Informed Graph

A third type of graph, namely the combination of WMG and GMG (CMG), is proposed in this work to simultaneously utilize WM and GM information for modeling anatomical relationships between clusters. Specifically, for each cluster (node) in CMG, its neighborhood clusters (nodes) are defined as clusters that both belong to the top k clusters with the lowest geometric distances and have the top two FreeSurfer regions in common.

2.3 Network Architecture

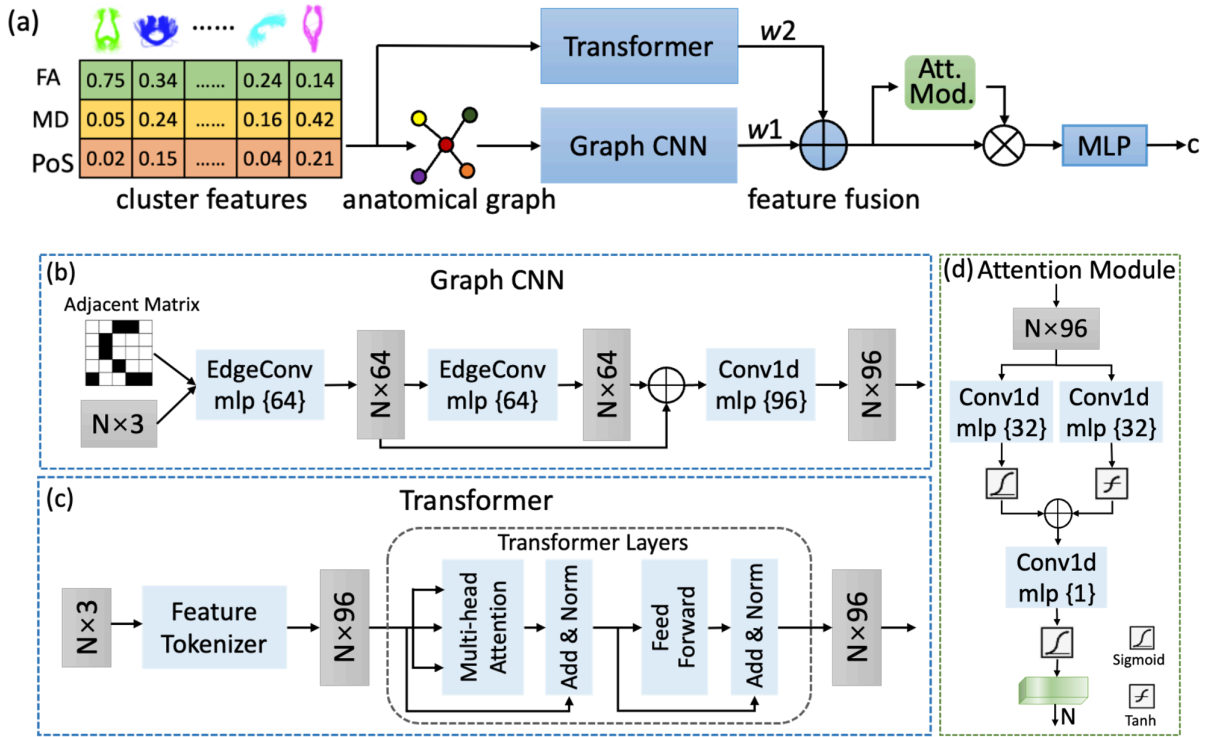


Fig. 2. (a) Overall pipeline of TractGraphFormer. (b) Network structure of the Graph CNN stream. (c) Network structure of the Transformer stream. (d) Network structure of the attention module. (N: number of clusters)

2.3.1 Overall Pipeline

The overall architecture of our proposed TractGraphFormer framework is shown in Fig. 2 (a). The proposed framework is a hybrid two-stream deep neural network incorporating Graph CNN and Transformer modules for feature extraction. Local and global features are extracted from the Graph CNN and the Transformer, respectively, and then these features are fused in a weighted sum manner. The Graph CNN stream extends the 1D-CNN model (He et al., 2022) for group classification using fiber cluster features by replacing the 1D convolutional layers in the original model with EdgeConv layers (Wang et al., 2019) to utilize the information of anatomically neighboring clusters (Section 2.3.2). We apply a Transformer (Gorishniy et al., 2021; Vaswani et al., 2017) with a self-attention mechanism that can naturally take each cluster as a token to

learn long-range dependencies among clusters (Section 2.3.3). After fusion of local and global features, we add a gated attention module (Ilse et al., 2018) in the network that can assess the importance of each cluster to enable interpretation of results (Section 2.3.4). Then a flatten operation and two fully-connected layers follow to obtain the final classification results.

2.3.2 Graph CNN Stream

In the Graph CNN stream, we adopt EdgeConv to aggregate information from neighboring nodes that represent anatomically similar fiber clusters (Fig. 3). EdgeConv was proposed in the popular DGCNN method to capture the local geometric structure of point clouds (Wang et al., 2019). The basic idea of EdgeConv is to use a learnable fully-connected layer to compute an edge feature of two neighboring nodes x_i and x_j based on their input features. Then, EdgeConv outputs the refined node features by aggregating the learned edge features with max-pooling. This learning process enables dynamic updates of graph structure by recomputing distances of points in the feature space. In our application, as the proposed graphs are built to explicitly reflect the anatomical relationship between fiber clusters, we maintain a static graph structure across layers by using the same graph structure across all EdgeConv layers without recomputing distances between node features.

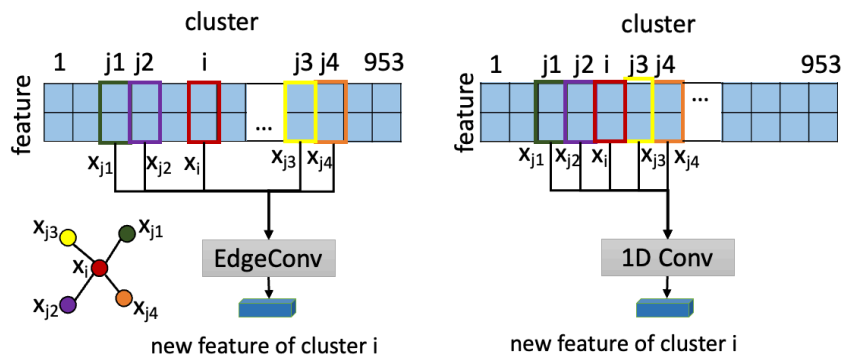


Fig. 3. Graphic illustration of the usage of EdgeConv to leverage fiber cluster neighborhood information, with comparison to the standard 1-D convolutional layer.

The overall architecture of the Graph CNN stream is shown in Fig. 2 (b). The inputs of Graph CNN are the constructed graphs (Section 2.2) including node (cluster) features and adjacency matrices defining edges between nodes. We use two EdgeConv layers and one 1-D convolutional layer to extract features. The two EdgeConv layers compute edge features with two fully-connected layers. Shortcut connections are included to extract multi-scale features and one 1-D convolutional layer (kernel size=1) is followed to aggregate multi-scale features obtained from the previous EdgeConv layers. Unlike general graphs, the nodes (clusters) in our constructed graph correspond across subjects. Therefore, after feature extraction, we do not use the max pooling operation as in traditional Graph CNNs, but instead, we retain the flatten operation in the 1D-CNN model (He et al., 2022) to preserve the information about cluster correspondence across subjects. The output of the Graph CNN stream is a feature matrix, where one dimension corresponds to clusters and the other dimension to the learned feature vector of each cluster.

2.3.3 Transformer Stream

Fig. 2 (c) illustrates the usage of the Transformer stream to capture long-range dependencies among cluster features. Specifically, the Transformer module used for feature extraction is adapted from the model in (Gorishniy et al., 2021), which is a simple adaptation of the vanilla Transformer architecture (Vaswani et al., 2017) for 1-D tabular data. As in (Gorishniy et al., 2021), a Transformer block comprises two parts, a feature tokenizer module and stacked Transformer layers, consisting of a self-attention and a feedforward module. For

our input data, we naturally take each cluster as a token and we get three features (FA, MD, and NoS) for each input token. Then, the feature tokenizer module transforms the input features into embeddings with a specified dimension. The embeddings are then input to the stacked Transformer layers to learn token features from all tokens. In each Transformer layer, the input features are first linearly mapped as query (Q), key (K), and value (V), which are the keys of the multi-head attention mechanism. The process is shown below (Vaswani et al., 2017):

$$[q, k, v] = xW_{qkv}, W_{qkv} \in R^{n \times d_{pkv}} \quad (1)$$

where n is the dimension of input embeddings for each token and d_{pkv} is the dimension of query/key/value. Then the output of the self-attention layer is computed as a weighted sum of the values, where the weight assigned to each value is computed by a compatibility function of the query with the corresponding key. The output attention map is calculated as (Vaswani et al., 2017):

$$Attention(Q, K, V) = softmax\left(\frac{QK^T}{\sqrt{d_k}}\right)V \quad (2)$$

where d_k is the dimension of key (Vaswani et al., 2017). Following that, a fully connected feed-forward network is applied to the obtained features of each token from the self-attention layer and generates the output features of the Transformer layer. The ‘‘classification token’’ in (Gorishniy et al., 2021) is removed from our model because the goal of the Transformer module is to extract global features for each token instead of obtaining a final classification score. In this way, the output of the Transformer module is a feature matrix, where one dimension corresponds to clusters and the other dimension corresponds to the learned feature vector of each cluster.

2.3.4 Fusion of Features from the Two-stream Model

After feature extraction from the Graph CNN and Transformer, respectively, we adopt a feature-level fusion strategy using a weighted sum to aggregate features from the two streams. Specifically, two learnable weights (w_1 and w_2) are assigned to the two streams and the fused features are calculated as the weighted sum of the features extracted from the Graph CNN and Transformer streams. The weights of the two streams are initialized and updated during model training to get the best classification performance.

2.3.5 Attention Module and Interpretation

For the purpose of interpretation, it is important to identify highly predictive WM connections for the task of sex classification. To achieve this, we add an attention mechanism after feature fusion using the popular gated attention module from (Ilse et al., 2018). The attention module (Fig. 2(d)) is composed of two parallel fully-connected layers followed by a sigmoid and tanh activation functions, a concatenation operation, and another fully-connected layer followed by a sigmoid function. The output is a 1-D attention map of size 953 with values between 0 and 1, indicating the importance of the corresponding cluster to the classification task. Thus at test time an attention score is obtained for each cluster in each subject.

Next, we identify the most predictive anatomical WM tracts. We first compute the mean score of each cluster across all testing subjects to identify a set of clusters that are highly predictive for the prediction task. Finally, we identify all tracts to which these predictive clusters belong, according to the ORG atlas (Zhang et al., 2018c).

2.3.6 Implementation Details

We adopt 5-fold cross-validation for model training and performance evaluation. In each fold, 7473 subjects (80%) of ABCD subjects are used for training the neural network, while 1869 (20%) are used for testing. For the HCP subjects, 852 subjects (80%) are used for training, while 213 (20%) are used for testing. The averaged prediction performance of all folds and standard deviation across folds are reported in the experimental results. We train and test each classification model on each dataset independently.

All experiments are performed on an NVIDIA RTX A4000 GPU using Pytorch (v1.12.1) (Paszke et al., 2019). Our overall network is trained for 100 epochs with a learning rate of 1e-3. The batch size of training is 32 and Adam (Kingma and Ba, 2014) is used for optimization. The number of selected WM-informed neighbors k is set to 30, which obtains the best performance in the parameter tuning experiment (see Section 3.1). For the Transformer module, the number of layers and number of heads are set to 1 considering the relatively small training dataset of medical images. The token dimension is 96, as well as the dimension of output features from the Graph CNN and Transformer streams. The weights of the two streams (w_1 and w_2) are initialized with 0.5.

3 Experiments and Results

We evaluate our proposed TractGraphFormer on a testbed task of sex classification on both ABCD and HCP datasets. First, we perform a parameter tuning experiment (Section 3.1). Second, we compare our proposed method with four state-of-the-art methods (Section 3.2). Third, we perform ablation studies to evaluate the effectiveness of each component of TractGraphFormer (Section 3.3). Finally, weights of Graph CNN and Transformer streams and highly predictive tracts for sex classification are identified for interpretation (Section 3.4) for both datasets.

Four evaluation metrics are adopted in our study to evaluate sex classification performance: accuracy, precision, recall and F1 score. For precision, recall, and F1 score, the averaged values of the two classes are calculated for evaluation.

3.1 Parameter Tuning Experiment

We investigated the influence of the number of white-matter-geometry-defined neighbors (k) on sex classification performance. We focus on CMG graph construction (see Section 2.2.3 for details). We explored the sex classification accuracies under five k values (10, 20, 30, 40, 50) for both datasets, as shown in Table 1. While the model performance is relatively robust to the choice of k , the performance of our model initially increases with the increase of k values, achieves a peak at $k=30$, and then decreases. This is likely because the aggregation of information from more anatomical neighbors benefits the performance gradually at first, but then the influence of distant clusters might mitigate the performance as the number of neighbors (k) increases.

Table 1 Accuracy across different numbers of neighbors (k) during graph construction for both datasets.

k	10	20	30	40	50
ABCD	85.50 (1.22)	85.81 (0.90)	86.25 (0.83)	85.99 (0.77)	86.01 (0.89)
HCP	94.46 (1.55)	94.84 (2.26)	95.59 (2.17)	95.31 (1.71)	94.84 (1.83)

3.2 State-of-the-art (SOTA) Comparison Experiments

We compared the performance of our proposed method with four SOTA methods: SVM, 1D-CNN (He et al., 2022), TractGraphCNN_{WMG}, and TractGraphCNN_{GMG}. SVM is one of the most commonly used machine learning algorithms for tractography-related classification tasks (Deng et al., 2019; Kim and Park, 2016; Zhang et al., 2018a). The 1D-CNN model in (He et al., 2022) was specifically proposed for sex classification and age prediction based on cluster-wise white matter features, and has demonstrated competitive performance. TractGraphCNN_{WMG} and TractGraphCNN_{GMG} are our preliminary work (Chen et al., 2023b) with two graph types, WMG and GMG, respectively. The parameters of each comparison method were fine-tuned to obtain the best performance. The sex classification results of all methods from the ABCD and HCP datasets are shown in Tables 2 and 3, respectively. To conduct statistical analysis on the results of evaluation metrics, a one-way repeated measures Analysis of Variance (ANOVA) was applied to each of the four evaluation metrics, followed by post-hoc pairwise comparisons using paired t-tests between our proposed method and each comparison method.

Table 2 Comparison of sex classification performance across methods and graph types for ABCD dataset.

Methods	Acc	Pre	Rec	F1
SVM	78.57 (2.07)***	78.61 (2.08)***	78.57 (2.00)***	78.52 (2.05)***
1D-CNN	84.22 (1.00)**	84.24 (1.05)**	84.14 (0.94)**	84.16 (0.98)**
TractGraphCNN _{WMG}	85.02 (1.32)*	85.04 (1.30)*	85.00 (1.23)*	84.98 (1.29)*
TractGraphCNN _{GMG}	85.17 (1.27)*	85.31 (1.54)*	85.05 (1.13)*	85.11 (1.21)
TractGraphFormer _{WMG}	86.09 (1.12)	86.16 (1.22)	86.03 (1.00)	86.05 (1.08)
TractGraphFormer _{GMG}	85.97 (1.12)	86.02 (1.03)	85.98 (1.04)	85.94 (1.10)
TractGraphFormer _{CMG}	86.25 (0.83)	86.29 (0.80)	86.21 (0.78)	86.21 (0.81)

p<0.0005*** p<0.005** p<0.05 *

Table 3 Comparison of sex classification performance across methods and graph types for HCP dataset.

Methods	Acc	Pre	Rec	F1
SVM	90.61 (2.83)***	90.52 (2.82)***	90.64 (2.91)***	90.55 (2.85)***
1D-CNN	92.58 (1.91)**	92.55 (1.90)**	92.59 (1.99)***	92.53 (1.93)**
TractGraphCNN _{WMG}	94.37 (2.75)*	94.34 (2.78)*	94.40 (2.70)*	94.33 (2.76)*
TractGraphCNN _{GMG}	94.27 (2.29)*	94.31 (2.22)*	94.31 (2.27)*	94.24 (2.29)*
TractGraphFormer _{WMG}	95.21 (1.96)	95.27 (1.94)	95.13 (1.98)	95.17 (1.97)
TractGraphFormer _{GMG}	94.84 (1.33)	94.79 (1.37)	94.86 (1.27)	94.80 (1.32)
TractGraphFormer _{CMG}	95.59 (2.17)	95.57 (2.22)	95.65 (2.10)	95.56 (2.17)

p<0.0005*** p<0.005** p<0.05 *

As shown in Tables 2 and 3, our proposed TractGraphFormer outperforms all comparison methods across both datasets, indicated by the highest values of all four evaluation metrics on classification accuracy. The ANOVA analyses show significant differences in the evaluation metrics of classification performance of compared methods for sex classification in both ABCD and HCP datasets (p<0.0001 in all analyses). In addition, post-hoc paired t-tests show that TractGraphFormer_{CMG} obtains significantly higher values than the

four comparison SOTA methods for all evaluation metrics across both datasets ($p < 0.05$ in all analyses, as indicated by asterisks in Tables 2 and 3).

We also compared the sex classification performance across the three proposed types of input graphs for the ABCD and HCP datasets, as shown in Tables 2 and 3. The results indicate that all graph types show competitive performance compared to SOTA methods, while CMG slightly outperforms WMG and GMG across both datasets. An ANOVA was performed among the evaluation metrics of the three graph types and discovered no significant difference. These results show that our proposed framework achieves good performance across three types of graphs, indicating the effectiveness of our network design in improving sex classification performance.

3.3 Ablation Studies

We performed ablation experiments to evaluate the contribution of various components to the overall TractGraphFormer framework. We investigated the classification performance of four models: TractGraphFormer, TractGraphFormer without attention module (TractGraphFormer w/o Att.), Graph CNN, and Transformer. An ANOVA analysis was applied to each of the four evaluation metrics. Then post-hoc pairwise comparisons using paired t-tests were performed between the evaluation metrics of different models.

As shown in Tables 4 and 5, the evaluation metrics of TractGraphFormer are higher than all compared models. The ANOVA analyses show significant differences in the evaluation metrics of compared models for sex classification across both datasets ($p < 0.0001$ in all analyses). The ablation study shows that the proposed TractGraphFormer architecture (with or without attention) significantly outperforms the basic Graph CNN or Transformer architectures. Therefore, the combination of Graph CNN and Transformer (TractGraphFormer) significantly improves classification performance compared to when only one stream is used for feature extraction. While the addition of attention slightly improves performance in both ABCD and HCP datasets, this is not significant; however, the added benefit of the attention module is that it can facilitate downstream interpretation.

Table 4 Ablation study of network components for the ABCD dataset.

Models	Acc	Pre	Rec	F1
Graph CNN	85.04 (1.08)**	85.09 (1.00)**	85.04 (0.98)**	85.01 (1.05)**
Transformer	85.43 (1.22)*	85.46 (1.23)*	85.37 (1.16)*	85.38 (1.20)*
TractGraphFormer w/o Att.	86.00 (0.92)	86.00 (0.91)	85.98 (0.90)	85.96 (0.91)
TractGraphFormer	86.25 (0.83)	86.29 (0.80)	86.21 (0.78)	86.21 (0.81)

$p < 0.005$ ** $p < 0.05$ *

Table 5 Ablation study of network components for the HCP dataset.

Models	Acc	Pre	Rec	F1
Graph CNN	94.65 (1.92)*	94.65 (1.89)*	94.57 (1.98)*	94.60 (1.94)*
Transformer	91.64 (1.61)***	91.85 (1.43)***	91.51 (1.51)***	91.56 (1.61)***
TractGraphFormer w/o Att.	95.40 (1.79)	95.41 (1.87)	95.35 (1.76)	95.35 (1.79)
TractGraphFormer	95.59 (2.17)	95.57 (2.22)	95.65 (2.10)	95.56 (2.17)

$p < 0.0005$ *** $p < 0.005$ ** $p < 0.05$ *

3.4 Interpretation results

3.4.1 Weights of Graph CNN and Transformer Streams

The weights of Graph CNN and Transformer streams (w_1 and w_2) during feature fusion were obtained from the trained models for both datasets. Within each fold, the two weights in the corresponding model were normalized to sum to 1. Both of the weights before (Weights) and after normalization (Weights_{norm}) were averaged across five folds and the results are shown in Table 6. As we can see, for the two datasets, both the Graph CNN and Transformer streams have noticeable weight values, indicating that both streams made substantial contributions to the final prediction results. For both datasets, the Graph CNN stream has larger weights than the Transformer stream. However, the contribution of the Transformer is larger in the ABCD than in HCP, indicated by larger normalized weights.

Table 6 Weights of Graph CNN and Transformer streams for feature fusion.

Dataset	ABCD		HCP	
	w_1	w_2	w_1	w_2
Weights	0.57 (0.05)	0.35 (0.16)	0.95 (0.07)	0.12 (0.04)
Weights _{norm}	0.63 (0.13)	0.37 (0.13)	0.89 (0.04)	0.11 (0.04)

3.4.2 Predictive White Matter Tracts

In this section, we enable visualization of white matter fiber tracts that were found to be highly predictive across both large datasets under study. Attention scores of each cluster were obtained from the attention module in TractGraphFormer for all testing subjects within each fold. Therefore, following the five-fold cross-validation experiments, we obtained attention scores for all subjects under study. For accurate interpretation of results, we only kept the attention scores of subjects whose sex category was correctly predicted. The predictive tracts for sex classification identified with our proposed interpretation method (see Section 2.3.4) for both datasets are listed in Table 7. Overall, we can observe that widespread regions in the WM are predictive of the sex of an individual. Some of the identified predictive tracts differ across datasets, as may be expected due to the developmental changes in white matter microstructure from childhood to young adulthood (Lebel et al., 2012). As shown in bold in Table 7 and visualized in Fig. 4, thirteen predictive tracts are consistently identified across the ABCD and HCP datasets. These include 5 thalamic projection tracts (bilateral thalamo-frontal, bilateral thalamo-temporal, and left thalamo-parietal) and 8 cortico-cortical association tracts (bilateral superior longitudinal fasciculus I, bilateral superficial frontal, left inferior longitudinal fasciculus, right middle longitudinal fascicle, right uncinate fasciculus, and right superficial parieto-temporal).

Table 7 Identified predictive tracts for sex classification for each dataset.

Dataset	ABCD	HCP
Tracts	CB_L, CB_R, ILF_L , ILF_R, MdLF_L, MdLF_R , SLF-I_L , SLF-I_R , SP_L, Sup-F_L , Sup-F_R , Sup-PT_L, Sup-PT_R , TF_L , TF_R , TP_L, TP_R, TT_L , TT_R , UF_L, UF_R	AF_L, CC1, CC2, CST_L, ICP_L, ILF_L , IOFF_L, Intra-CBLM-PaT_L, Intra-CBLM-PaT_R, MdLF_R , SF_L, SF_R, SLF-II_L, SLF-II_R, SLF-I_L , SLF-I_R , SO_L, Sup-FP_L, Sup-FP_R, Sup-F_L , Sup-F_R , Sup-PT_R , Sup-P_L, Sup-P_R, TF_L , TF_R , TP_L , TT_L , TT_R , UF_R

AF: arcuate fasciculus; CB: cingulum bundle; CC: corpus callosum; CST: corticospinal tract; ICP: inferior cerebellar peduncle; ILF: inferior longitudinal fasciculus; IOFF: inferior occipito-frontal fasciculus; Intra-CBLM-PaT: intracerebellar parallel tract; MdLF: middle longitudinal fasciculus; SF: striato-frontal; SLF: superior longitudinal fasciculus; SO: striato-occipital; SP: striato-parietal; Sup-F: superficial-frontal; Sup-FP:

superficial-frontal-parietal; Sup-P: superficial-parietal; Sup-PT: superficial-parietal-temporal; TF: thalamo-frontal; TP: thalamo-parietal; TT: thalamo-temporal; UF: uncinate fasciculus

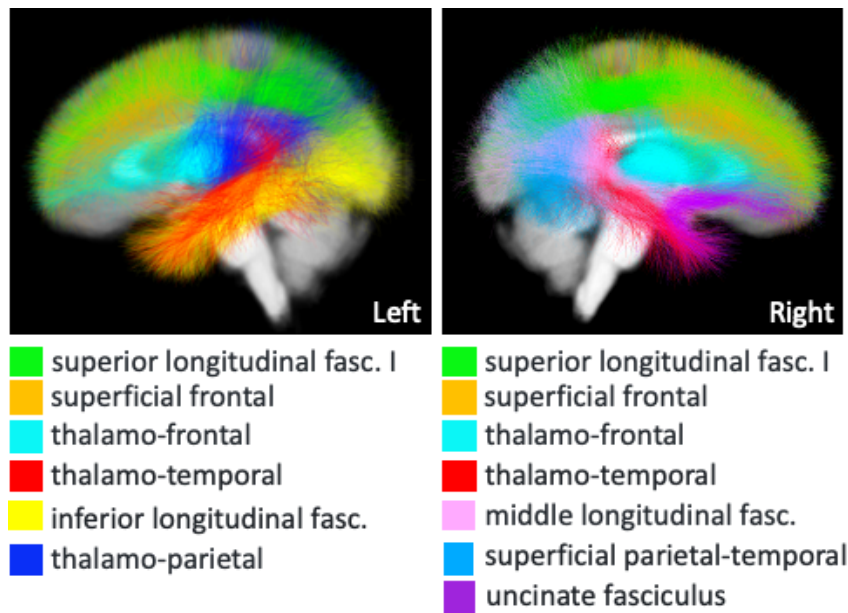


Fig. 4. Visualization of predictive tracts commonly identified across both ABCD and HCP datasets.

4 Discussion

In this work, we propose a novel hybrid deep learning framework, TractGraphFormer, for group classification based on cluster-wise white matter features from dMRI tractography. TractGraphFormer is a two-stream deep neural network consisting of a parallel Graph CNN and Transformer feature extractor. In the Graph CNN stream, anatomically informed local features are learned by modeling the anatomical relationship between clusters as a graph. The Transformer with a self-attention mechanism extracts global features from all clusters by taking each cluster as a token. Then the local and global features are fused for classification, and an attention module enables interpretation of predictive tracts for the classification results. Our proposed method demonstrates superior performance compared to SOTA methods through evaluation on two large-scale datasets. Ablation studies show that the aggregation of anatomically informed local and global information significantly improves classification performance. A set of predictive tracts for sex classification were successfully identified for both datasets with our method.

Our proposed TractGraphFormer framework has demonstrated superior sex prediction performance compared to several SOTA methods, which used the same inputs as ours. However, the studies that adopted the same inputs as ours are limited. To further demonstrate the effectiveness of our approach in achieving accurate sex classification, we broaden our literature review to evaluate our performance in comparison to previous studies that use different white matter features such as structural connectivity. Though the direct comparison of performance is difficult due to the difference in input features, our method demonstrates competitive sex classification performance compared to existing studies in the literature. For example, a recent study of sex prediction from HCP structural connectivity data achieved 92.75% accuracy (Shanthamallu et al., 2019) and the well-known BrainNetCNN achieved 76.5% accuracy in a study of 3,152 participants (Yeung et al., 2020).

By comparing the sex prediction performance across the ABCD and HCP datasets, we observe that HCP obtains obviously higher classification performance than ABCD. Considering that the subjects of ABCD and HCP datasets belong to different age groups (adolescents for ABCD and young adults for HCP), the

classification performance differences between the two datasets could be related to the developmental differences in white matter between males and females from adolescence to adulthood, which have been demonstrated by previous studies (De Bellis et al., 2001; Lebel et al., 2012; Schmithorst et al., 2008).

Our method is designed to improve performance by utilizing anatomical information that is encoded in a graph. As anatomical information, we leverage WM geometry and GM connectivity information, which have previously been shown to be useful for dMRI-based statistical analyses and machine learning prediction tasks (Yeung et al., 2023; Zhang et al., 2018b). We build graphs where neighborhoods are defined using the anatomical information, and we adopt EdgeConv modules to aggregate features from neighboring clusters. EdgeConv (Wang et al., 2019) has previously been shown to successfully aggregate features from neighboring nodes defined in a graph (Astolfi et al., 2020; Chen et al., 2023a; Xue et al., 2023). We attribute the improved performance of our proposed graph-based networks to their ability to learn information from neighboring nodes with related anatomy. This is similar to how, in image processing, a CNN can leverage information from neighboring pixels with similar image information. In contrast, the raw cluster-wise white matter features are in no particular order, so the compared 1D-CNN method applies convolutions that combine information from anatomically different fiber clusters. The proposed graph design is also robust as it is relatively insensitive to the number of chosen neighbors in the graph. As expected, with increasing k values, the prediction performance first increases due to integrating information from nearby clusters and then decreases due to including more information from distant clusters. The experimental results support our hypothesis that deep learning performance can be enhanced by incorporating information about white matter geometry and gray matter connectivity, particularly about neighborhoods of nearby and anatomically similar fiber tracts. Our results confirm the overall effectiveness of our graph model, which incorporates anatomical information to guide convolutions.

The proposed hybrid Graph CNN and Transformer framework learns local and global features simultaneously to boost prediction performance. In the computer vision community, Transformers are well known to be capable of capturing long-range dependencies, thus benefiting prediction performance (Cao et al., 2023; Lu et al., 2022; Sarasua et al., 2022; Zhang et al., 2022c). In parallel to the Graph CNN, we add a Transformer module to extract global features from all clusters, providing a supplement to the local features learned from the Graph CNN. The strategy of combining local and global information to improve performance has demonstrated success in various computer vision applications (Fang et al., 2022; A. He et al., 2023). Our experimental results show that using only the Graph CNN or Transformer stream can achieve reasonable sex prediction performance; however, the combination of the two streams can further improve performance significantly, due to the learned complementary local and global information. The interpretation results about the weights of the Graph CNN and Transformer streams further demonstrate that both streams contributed to the prediction results for both datasets. The Graph CNN stream plays a more important role in prediction, indicating that local features from anatomically neighboring clusters are more informative for the sex prediction task. The Transformer is more important for the ABCD dataset than the HCP dataset, potentially due to the fact that good Transformer performance requires large-scale training data (Yuan et al., 2021), so the Transformer is more helpful for the much larger ABCD dataset.

The adoption of an attention module enables the interpretation of predictive tracts for sex prediction tasks while slightly improving prediction performance. The interpretation of predictive tracts can allow further investigation of the relationship between sex differences and white matter connections. Several of the tracts that were found to be predictive for sex classification across the HCP and ABCD datasets have long been known to exhibit sex differences, including the inferior longitudinal fasciculus, superior longitudinal fasciculus, uncinate fasciculus, and thalamo-frontal connections (Choi et al., 2010; Jung et al., 2019; Kitamura et al., 2011). Though the effects of sex on the superficial white matter are less studied, our method identified the superficial parietal-temporal tract as an predictive tract for sex prediction. This is in accordance with one previous study

that discovered sex differences in FA in the superficial white matter in temporoparietal regions (Phillips et al., 2013). While our main focus in this study was on network design using anatomical information, we believe this is the largest data-driven assessment of tracts that may be predictive for sex classification, focusing on those that are in common across two large datasets.

Finally, we note some limitations of this study and directions for future research. First, we evaluated our proposed method on data with popular dMRI research acquisition protocols using the UKFt tractography method, which provided fiber-specific FA and MD microstructure measures. It is of future interest to further demonstrate the applicability of our method to other types of input data including different dMRI acquisitions, tractography algorithms, and WM features. (We note that this work is resource-intensive, as generation of the ABCD dataset employed here required about 50,000 CPU hours (Cetin-Karayumak et al., 2024).) Second, future work may investigate the utility of incorporating other anatomical relationships, such as the proximity or connectivity of gray matter regions, to enhance network design for the analysis of additional types of brain morphometric data such as cortical volume or thickness. Furthermore, in the current work, we evaluated our method on a testbed class of sex classification using dMRI data from two large datasets of different ages. Future work could investigate the performance of our method on additional prediction tasks or on data from other groups such as those related to aging or disease. Future work could also move beyond a binary prediction of sex to conceptualize sex along a continuum (Phillips et al., 2019; Sanchis-Segura et al., 2022). Finally, in the current work, we utilized a straightforward weighted sum strategy to fuse learned local and global features. Future work could explore more advanced feature fusion methods that may further improve prediction performance (Han et al., 2023).

5 Conclusion

In conclusion, we propose an anatomically informed hybrid Graph CNN and Transformer model for machine learning with diffusion MRI tractography. This model combines Graph CNN and Transformer architectures to capture robust local and global features by leveraging anatomical relationships and long-range interactions. It demonstrates strong performance in a sex prediction task across two large datasets. An attention module helps identify important tracts for accurate sex prediction, showing that widespread WM tracts are predictive and consistent across datasets. These include thalamic projection tracts (bilateral thalamo-frontal and thalamo-temporal, and left thalamo-parietal) and association tracts (bilateral superior longitudinal fasciculus I and superficial frontal, left inferior longitudinal fasciculus, and right middle longitudinal fascicle, uncinate fasciculus, and superficial parieto-temporal). This approach highlights the potential of incorporating local anatomical information and global feature dependencies for improved prediction performance in machine learning using dMRI tractography.

Declaration of Generative AI and AI-assisted technologies in the writing process

During the preparation of this work the authors used ChatGPT in order to improve the readability of several paragraphs in the Introduction. After using this tool/service, the authors reviewed and edited the content as needed and took full responsibility for the content of the publication.

Data and code availability

The ABCD and HCP datasets used in this project can be downloaded through the ABCD Study (<https://abcdstudy.org/>) and ConnectomeDB (db.humanconnectome.org) websites. The harmonized dMRI data, extracted white matter clusters, and microstructure measures from the ABCD study are available through the NIMH Data Archive (NDA) repository (https://nda.nih.gov/edit_collection.html?id=3371) (Cetin-Karayumak et

al., 2024). The code for data analysis will be available upon publication at <https://github.com/AnnabelChen51/TractGraphFormer>.

Author contributions

Yuqian Chen: Conceptualization, Methodology, Software, Writing - Original draft preparation. Fan Zhang: Conceptualization, Methodology, Writing - Review & Editing. Meng Wang: Methodology, Writing - Review & Editing. Leo R. Zekelman: Data Curation, Writing - Draft and Editing. Suheyla Cetin-Karayumak: Data Curation. Tengfei Xue: Methodology, Writing- Reviewing and Editing. Chaoyi Zhang: Methodology, Writing- Reviewing and Editing. Yang Song: Writing- Reviewing and Editing. Nikos Makris: Conceptualization, Writing- Reviewing and Editing. Yogesh Rathi: Writing- Reviewing and Editing. Weidong Cai: Resources, Supervision, Writing- Reviewing and Editing. Lauren J. O'Donnell: Conceptualization, Methodology, Writing - Review & Editing, Supervision, Funding acquisition.

Acknowledgments

This work was supported by the National Institutes of Health (NIH) grants: R01MH132610, R01MH125860, R01MH119222, R01MH116173, P41EB015902, R01NS125307, R01NS125781, R01MH112748, R01AG042512, and K24MH116366; the National Key R&D Program of China (No. 2023YFE0118600); the National Natural Science Foundation of China (No. 62371107).

References

- Astolfi, P., Verhagen, R., Petit, L., Olivetti, E., Masci, J., Boscaini, D., Avesani, P., 2020. Tractogram Filtering of Anatomically Non-plausible Fibers with Geometric Deep Learning, in: *Medical Image Computing and Computer Assisted Intervention – MICCAI 2020*. Springer International Publishing, pp. 291–301.
- Cao, H., Wang, Y., Chen, J., Jiang, D., Zhang, X., Tian, Q., Wang, M., 2023. Swin-Unet: Unet-Like Pure Transformer for Medical Image Segmentation, in: *Computer Vision – ECCV 2022 Workshops*. Springer Nature Switzerland, pp. 205–218.
- Casey, B.J., Cannonier, T., Conley, M.I., Cohen, A.O., Barch, D.M., Heitzeg, M.M., Soules, M.E., Teslovich, T., Dellarco, D.V., Garavan, H., Orr, C.A., Wager, T.D., Banich, M.T., Speer, N.K., Sutherland, M.T., Riedel, M.C., Dick, A.S., Bjork, J.M., Thomas, K.M., Chararani, B., Mejia, M.H., Hagler, D.J., Jr, Daniela Cornejo, M., Sicut, C.S., Harms, M.P., Dosenbach, N.U.F., Rosenberg, M., Earl, E., Bartsch, H., Watts, R., Polimeni, J.R., Kuperman, J.M., Fair, D.A., Dale, A.M., ABCD Imaging Acquisition Workgroup, 2018. The Adolescent Brain Cognitive Development (ABCD) study: Imaging acquisition across 21 sites. *Dev. Cogn. Neurosci.* 32, 43–54.
- Cetin-Karayumak, S., Zhang, F., Zurrin, R., Billah, T., Zekelman, L., Makris, N., Pieper, S., O'Donnell, L.J., Rathi, Y., 2024. Harmonized diffusion MRI data and white matter measures from the Adolescent Brain Cognitive Development Study. *Sci Data* 11, 249.
- Chen, J., Bayanagari, V.L., Chung, S., Wang, Y., Lui, Y.W., 2024. Deep learning with diffusion MRI as in vivo microscope reveals sex-related differences in human white matter microstructure. *Sci. Rep.* 14, 9835.
- Chen, M., Li, H., Wang, J., Yuan, W., Altaye, M., Parikh, N.A., He, L., 2020. Early Prediction of Cognitive Deficit in Very Preterm Infants Using Brain Structural Connectome With Transfer Learning Enhanced Deep Convolutional Neural Networks. *Front. Neurosci.* 14. <https://doi.org/10.3389/fnins.2020.00858>
- Chen, Y., Zekelman, L.R., Zhang, C., Xue, T., Song, Y., Makris, N., Rathi, Y., Golby, A.J., Cai, W., Zhang, F., O'Donnell, L.J., 2024. TractGeoNet: A geometric deep learning framework for pointwise analysis of tract microstructure to predict language assessment performance. *Med. Image Anal.* 103120.
- Chen, Y., Zhang, C., Xue, T., Song, Y., Makris, N., Rathi, Y., Cai, W., Zhang, F., O'Donnell, L.J., 2023a. Deep fiber clustering: Anatomically informed fiber clustering with self-supervised deep learning for fast and effective tractography parcellation. *Neuroimage* 273, 120086.
- Chen, Y., Zhang, F., Zekelman, L.R., Xue, T., Zhang, C., Song, Y., Makris, N., Rathi, Y., Cai, W., O'Donnell, L.J., 2023b. Tractgraphcnn: Anatomically Informed Graph CNN for Classification Using Diffusion MRI Tractography, in: *2023 IEEE 20th International Symposium on Biomedical Imaging (ISBI)*. IEEE, pp. 1–5.
- Chen, Y., Zhang, F., Zhang, C., Xue, T., Zekelman, L.R., He, J., Song, Y., Makris, N., Rathi, Y., Golby, A.J., Cai, W., O'Donnell, L.J., 2022. White Matter Tracts are Point Clouds: Neuropsychological Score Prediction and Critical Region Localization via Geometric Deep Learning, in: *Medical Image Computing and Computer Assisted Intervention – MICCAI 2022*. Springer Nature Switzerland, pp. 174–184.
- Choi, C.-H., Lee, J.-M., Koo, B.-B., Park, J.S., Kim, D.-S., Kwon, J.S., Kim, I.Y., 2010. Sex differences in the temporal lobe white matter and the corpus callosum: a diffusion tensor tractography study. *Neuroreport* 21, 73–77.
- De Bellis, M.D., Keshavan, M.S., Beers, S.R., Hall, J., Frustaci, K., Masalehdan, A., Noll, J., Boring, A.M., 2001. Sex differences in brain maturation during childhood and adolescence. *Cereb. Cortex* 11, 552–557.
- Deng, Y., Hung, K.S.Y., Lui, S.S.Y., Chui, W.W.H., Lee, J.C.W., Wang, Y., Li, Z., Mak, H.K.F., Sham, P.C., Chan, R.C.K., Cheung, E.F.C., 2019. Tractography-based classification in distinguishing patients with first-episode schizophrenia from healthy individuals. *Prog. Neuropsychopharmacol. Biol. Psychiatry* 88, 66–73.
- Descoteaux, M., Angelino, E., Fitzgibbons, S., Deriche, R., 2007. Regularized, fast, and robust analytical Q-ball imaging. *Magn. Reson. Med.* 58, 497–510.
- Dosovitskiy, A., Beyer, L., Kolesnikov, A., Weissenborn, D., Zhai, X., Unterthiner, T., Dehghani, M., Minderer, M., Heigold, G., Gelly, S., Uszkoreit, J., Houlsby, N., 2021. An image is worth 16x16 words: Transformers for image recognition at scale, in: *International Conference on Learning Representations 2021*. Presented at the International Conference on Learning Representations.
- Eikenes, L., Visser, E., Vangberg, T., Håberg, A.K., 2022. Both brain size and biological sex contribute to variation in white matter microstructure in middle-aged healthy adults. *Hum. Brain Mapp.*

<https://doi.org/10.1002/hbm.26093>

- Fang, J., Lin, H., Chen, X., Zeng, K., 2022. A hybrid network of cnn and transformer for lightweight image super-resolution, in: *Proceedings of the IEEE/CVF Conference on Computer Vision and Pattern Recognition*. pp. 1103–1112.
- Farquharson, S., Tournier, J.-D., Calamante, F., Fabinyi, G., Schneider-Kolsky, M., Jackson, G.D., Connelly, A., 2013. White matter fiber tractography: why we need to move beyond DTI. *J. Neurosurg.* 118, 1367–1377.
- Feng, G., Wang, Y., Huang, W., Chen, H., Dai, Z., Ma, G., Li, X., Zhang, Z., Shu, N., 2022. Methodological evaluation of individual cognitive prediction based on the brain white matter structural connectome. *Hum. Brain Mapp.* 43, 3775–3791.
- Fischl, B., 2012. FreeSurfer. *Neuroimage* 62, 774–781.
- Forkel, S.J., Friedrich, P., Thiebaut de Schotten, M., Howells, H., 2022. White matter variability, cognition, and disorders: a systematic review. *Brain Struct. Funct.* 227, 529–544.
- Gabusi, I., Battocchio, M., Bosticardo, S., Schiavi, S., Daducci, A., 2024. Blurred streamlines: A novel representation to reduce redundancy in tractography. *Med. Image Anal.* 93, 103101.
- Garyfallidis, E., Côté, M.-A., Rheault, F., Sidhu, J., Hau, J., Petit, L., Fortin, D., Cunanne, S., Descoteaux, M., 2018. Recognition of white matter bundles using local and global streamline-based registration and clustering. *Neuroimage* 170, 283–295.
- Gong, W., Beckmann, C.F., Smith, S.M., 2021. Phenotype discovery from population brain imaging. *Med. Image Anal.* 71, 102050.
- Gorishniy, Y., Rubachev, I., Khrulkov, V., Babenko, A., 2021. Revisiting deep learning models for tabular data. *Adv. Neural Inf. Process. Syst.* 34, 18932–18943.
- Han, Z., Zhang, C., Fu, H., Zhou, J.T., 2023. Trusted Multi-View Classification With Dynamic Evidential Fusion. *IEEE Trans. Pattern Anal. Mach. Intell.* 45, 2551–2566.
- He, A., Wang, K., Li, T., Du, C., Xia, S., Fu, H., 2023. H2Former: An Efficient Hierarchical Hybrid Transformer for Medical Image Segmentation. *IEEE Trans. Med. Imaging* 42, 2763–2775.
- He, H., Zhang, F., Pieper, S., Makris, N., Rathi, Y., Wells, W., O'Donnell, L.J., 2022. Model and Predict Age and Sex in Healthy Subjects Using Brain White Matter Features: A Deep Learning Approach, in: *2022 IEEE 19th International Symposium on Biomedical Imaging (ISBI)*. ieeexplore.ieee.org, pp. 1–5.
- He, J., Zhang, F., Pan, Y., Feng, Y., Rushmore, J., Torio, E., Rathi, Y., Makris, N., Kikinis, R., Golby, A.J., O'Donnell, L.J., 2023. Reconstructing the somatotopic organization of the corticospinal tract remains a challenge for modern tractography methods. *Hum. Brain Mapp.* 44, 6055–6073.
- Ilse, M., Tomczak, J., Welling, M., 2018. Attention-based Deep Multiple Instance Learning, in: Dy, J., Krause, A. (Eds.), *ICML, Proceedings of Machine Learning Research*. PMLR, pp. 2127–2136.
- Ingalhalikar, M., Smith, A., Parker, D., Satterthwaite, T.D., Elliott, M.A., Ruparel, K., Hakonarson, H., Gur, R.E., Gur, R.C., Verma, R., 2014. Sex differences in the structural connectome of the human brain. *Proc. Natl. Acad. Sci. U. S. A.* 111, 823–828.
- Jeong, J.-W., Lee, M.-H., O'Hara, N., Juhász, C., Asano, E., 2021. Prediction of baseline expressive and receptive language function in children with focal epilepsy using diffusion tractography-based deep learning network. *Epilepsy Behav.* 117, 107909.
- Jung, M., Mody, M., Fujioka, T., Kimura, Y., Okazawa, H., Kosaka, H., 2019. Sex Differences in White Matter Pathways Related to Language Ability. *Front. Neurosci.* 13, 898.
- Kawahara, J., Brown, C.J., Miller, S.P., Booth, B.G., Chau, V., Grunau, R.E., Zwicker, J.G., Hamarneh, G., 2017. BrainNetCNN: Convolutional neural networks for brain networks; towards predicting neurodevelopment. *Neuroimage* 146, 1038–1049.
- Kim, M., Park, H., 2016. Using Tractography to Distinguish SWEDD from Parkinson's Disease Patients Based on Connectivity. *Parkinsons Dis.* 2016, 8704910.
- Kingma, D.P., Ba, J., 2014. Adam: A Method for Stochastic Optimization. *arXiv [cs.LG]*.
- Kitamura, S., Morikawa, M., Kiuchi, K., Taoka, T., Fukusumi, M., Kichikawa, K., Kishimoto, T., 2011. Asymmetry, sex differences and age-related changes in the white matter in the healthy elderly: a tract-based study. *BMC Res. Notes* 4, 378.
- Ktena, S.I., Parisot, S., Ferrante, E., Rajchl, M., Lee, M., Glocker, B., Rueckert, D., 2018. Metric learning with spectral graph convolutions on brain connectivity networks. *Neuroimage* 169, 431–442.
- Kulkarni, V., Pudipeddi, J.S., Akoglu, L., Vogelstein, J.T., Vogelstein, R.J., Ryman, S., Jung, R.E., 2013. Sex

- Differences in the Human Connectome, in: *Brain and Health Informatics*. Springer International Publishing, pp. 82–91.
- Lebel, C., Gee, M., Camicioli, R., Wieler, M., Martin, W., Beaulieu, C., 2012. Diffusion tensor imaging of white matter tract evolution over the lifespan. *Neuroimage* 60, 340–352.
- Liu, R., Li, M., Dunson, D.B., 2023. PPA: Principal parcellation analysis for brain connectomes and multiple traits. *Neuroimage* 276, 120214.
- Liu, W., Chen, Y., Ye, C., Makris, N., Rathi, Y., Cai, W., Zhang, F., O'Donnell, L.J., 2023. Fiber Tract Shape Measures Inform Prediction of Non-Imaging Phenotypes. *arXiv [cs.CV]*.
- Lo, Y., Chen, Y., Liu, D., Liu, W., Zekelman, L., Zhang, F., Rathi, Y., Makris, N., Golby, A.J., Cai, W., O'Donnell, L.J., 2024. Cross-domain Fiber Cluster Shape Analysis for Language Performance Cognitive Score Prediction. *ArXiv*.
- Lu, Y., Fu, J., Li, X., Zhou, W., Liu, S., Zhang, X., Wu, W., Jia, C., Liu, Y., Chen, Z., 2022. RTN: Reinforced Transformer Network for Coronary CT Angiography Vessel-level Image Quality Assessment, in: *Medical Image Computing and Computer Assisted Intervention – MICCAI 2022*. Springer Nature Switzerland, pp. 644–653.
- Machado-Reyes, D., Kim, M., Chao, H., Shen, L., Yan, P., 2022. Connectome transformer with anatomically inspired attention for Parkinson's diagnosis, in: *Proceedings of the 13th ACM International Conference on Bioinformatics, Computational Biology and Health Informatics, BCB '22*. Association for Computing Machinery, New York, NY, USA, pp. 1–4.
- Ning, L., Laun, F., Gur, Y., DiBella, E.V.R., Deslauriers-Gauthier, S., Megherbi, T., Ghosh, A., Zucchelli, M., Menegaz, G., Fick, R., St-Jean, S., Paquette, M., Aranda, R., Descoteaux, M., Deriche, R., O'Donnell, L., Rathi, Y., 2015. Sparse Reconstruction Challenge for diffusion MRI: Validation on a physical phantom to determine which acquisition scheme and analysis method to use? *Med. Image Anal.* 26, 316–331.
- Norton, I., Essayed, W.I., Zhang, F., Pujol, S., Yarmarkovich, A., Golby, A.J., Kindlmann, G., Wassermann, D., Estepar, R.S.J., Rathi, Y., Pieper, S., Kikinis, R., Johnson, H.J., Westin, C.-F., O'Donnell, L.J., 2017. SlicerDMRI: Open Source Diffusion MRI Software for Brain Cancer Research. *Cancer Res.* 77, e101–e103.
- O'Donnell, L.J., Westin, C.-F., 2007. Automatic Tractography Segmentation Using a High-Dimensional White Matter Atlas. *IEEE Trans. Med. Imaging* 26, 1562–1575.
- Park, H.-J., Friston, K., 2013. Structural and functional brain networks: from connections to cognition. *Science* 342, 1238411.
- Paszke, A., Gross, S., Massa, F., Lerer, A., Bradbury, J., Chanan, G., Killeen, T., Lin, Z., Gimelshein, N., Antiga, L., Desmaison, A., Kopf, A., Yang, E., DeVito, Z., Raison, M., Tejani, A., Chilamkurthy, S., Steiner, B., Fang, L., Bai, J., Chintala, S., 2019. PyTorch: An Imperative Style, High-Performance Deep Learning Library, in: Wallach, H., Larochelle, H., Beygelzimer, A., d'Alché-Buc, F., Fox, E., Garnett, R. (Eds.), *Advances in Neural Information Processing Systems*. Curran Associates, Inc.
- Phillips, O.R., Clark, K.A., Luders, E., Azhir, R., Joshi, S.H., Woods, R.P., Mazziotta, J.C., Toga, A.W., Narr, K.L., 2013. Superficial white matter: effects of age, sex, and hemisphere. *Brain Connect.* 3, 146–159.
- Phillips, O.R., Onopa, A.K., Hsu, V., Ollila, H.M., Hillary, R.P., Hallmayer, J., Gotlib, I.H., Taylor, J., Mackey, L., Singh, M.K., 2019. Beyond a Binary Classification of Sex: An Examination of Brain Sex Differentiation, Psychopathology, and Genotype. *J. Am. Acad. Child Adolesc. Psychiatry* 58, 787–798.
- Reddy, C.P., Rathi, Y., 2016. Joint Multi-Fiber NODDI Parameter Estimation and Tractography Using the Unscented Information Filter. *Front. Neurosci.* 10, 166.
- Sanchis-Segura, C., Aguirre, N., Cruz-Gómez, Á.J., Félix, S., Forn, C., 2022. Beyond “sex prediction”: Estimating and interpreting multivariate sex differences and similarities in the brain. *Neuroimage* 257, 119343.
- Sarasua, I., Pölsterl, S., Wachinger, C., 2022. CASHformer: Cognition Aware SHape Transformer for Longitudinal Analysis, in: *Medical Image Computing and Computer Assisted Intervention – MICCAI 2022*. Springer Nature Switzerland, pp. 44–54.
- Schmithorst, V.J., Holland, S.K., Dardzinski, B.J., 2008. Developmental differences in white matter architecture between boys and girls. *Hum. Brain Mapp.* 29, 696–710.
- Shanthamallu, U., Li, Q., Thiagarajan, J.J., Anirudh, R., Bremer, P.T., 2019. Modeling human brain connectomes using structured neural networks [WWW Document]. URL

<https://www.osti.gov/servlets/purl/1579625> (accessed 11.10.22).

- Van Essen, D.C., Smith, S.M., Barch, D.M., Behrens, T.E.J., Yacoub, E., Ugurbil, K., WU-Minn HCP Consortium, 2013. The WU-Minn Human Connectome Project: an overview. *Neuroimage* 80, 62–79.
- Vaswani, A., Shazeer, N., Parmar, N., Uszkoreit, J., Jones, L., Gomez, A.N., Kaiser, Ł., Polosukhin, I., 2017. Attention is All you Need. *Adv. Neural Inf. Process. Syst.* 30.
- Vos, S.B., Viergever, M.A., Leemans, A., 2013. Multi-fiber tractography visualizations for diffusion MRI data. *PLoS One* 8, e81453.
- Wang, Y., Sun, Y., Liu, Z., Sarma, S.E., Bronstein, M.M., Solomon, J.M., 2019. Dynamic Graph CNN for Learning on Point Clouds. *ACM Trans. Graph.* 38, 1–12.
- Wei, Y., Chen, Y., Xue, T., Zekelman, L., Makris, N., Rathi, Y., Cai, W., Zhang, F., O'Donnell, L.J., 2023. A Deep Network for Explainable Prediction of Non-imaging Phenotypes Using Anatomical Multi-view Data, in: *Computational Diffusion MRI*. Springer Nature Switzerland, pp. 165–176.
- Wu, H., Xiao, B., Codella, N., Liu, M., Dai, X., Yuan, L., Zhang, L., 2021. CvT: Introducing convolutions to vision transformers, in: *2021 IEEE/CVF International Conference on Computer Vision (ICCV)*. Presented at the 2021 IEEE/CVF International Conference on Computer Vision (ICCV), IEEE, pp. 22–31.
- Xue, T., Chen, Y., Zhang, C., Golby, A.J., Makris, N., Rathi, Y., Cai, W., Zhang, F., O'Donnell, L.J., 2023. TractCloud: Registration-Free Tractography Parcellation with a Novel Local-Global Streamline Point Cloud Representation, in: *Medical Image Computing and Computer Assisted Intervention – MICCAI 2023*. Springer Nature Switzerland, pp. 409–419.
- Xue, T., Zhang, F., Zekelman, L.R., Zhang, C., Chen, Y., Cetin-Karayumak, S., Pieper, S., Wells, W.M., Rathi, Y., Makris, N., Cai, W., O'Donnell, L.J., 2024. TractoSCR: a novel supervised contrastive regression framework for prediction of neurocognitive measures using multi-site harmonized diffusion MRI tractography. *Front. Neurosci.* 18. <https://doi.org/10.3389/fnins.2024.1411797>
- Yeung, H.W., Luz, S., Cox, S.R., Buchanan, C.R., Whalley, H.C., Smith, K.M., 2020. Pipeline comparisons of convolutional neural networks for structural connectomes: predicting sex across 3,152 participants. *Conf. Proc. IEEE Eng. Med. Biol. Soc.* 2020, 1692–1695.
- Yeung, H.W., Stolicyn, A., Buchanan, C.R., Tucker-Drob, E.M., Bastin, M.E., Luz, S., McIntosh, A.M., Whalley, H.C., Cox, S.R., Smith, K., 2023. Predicting sex, age, general cognition and mental health with machine learning on brain structural connectomes. *Hum. Brain Mapp.* 44, 1913–1933.
- Yuan, K., Guo, S., Liu, Z., Zhou, A., Yu, F., Wu, W., 2021. Incorporating convolution designs into visual transformers, in: *2021 IEEE/CVF International Conference on Computer Vision (ICCV)*. Presented at the 2021 IEEE/CVF International Conference on Computer Vision (ICCV), IEEE. <https://doi.org/10.1109/iccv48922.2021.00062>
- Zekelman, L.R., Zhang, F., Makris, N., He, J., Chen, Y., Xue, T., Liera, D., Drane, D.L., Rathi, Y., Golby, A.J., O'Donnell, L.J., 2022. White matter association tracts underlying language and theory of mind: An investigation of 809 brains from the Human Connectome Project. *Neuroimage* 246, 118739.
- Zhang, F., Cetin-Karayumak, S., Pieper, S., Rathi, Y., O'Donnell, L.J., 2022a. Consistent White Matter Parcellation in Adolescent Brain Cognitive Development (ABCD): A ~10k Harmonized Diffusion MRI Study, in: *Annual Meeting of the International Society for Magnetic Resonance in Medicine – ISMRM 2022*. Presented at the ISMRM 2022.
- Zhang, F., Daducci, A., He, Y., Schiavi, S., Seguin, C., Smith, R.E., Yeh, C.-H., Zhao, T., O'Donnell, L.J., 2022b. Quantitative mapping of the brain's structural connectivity using diffusion MRI tractography: A review. *Neuroimage* 249, 118870.
- Zhang, F., Noh, T., Juvekar, P., Frisken, S.F., Rigolo, L., Norton, I., Kapur, T., Pujol, S., Wells, W., 3rd, Yarmarkovich, A., Kindlmann, G., Wassermann, D., San Jose Estepar, R., Rathi, Y., Kikinis, R., Johnson, H.J., Westin, C.-F., Pieper, S., Golby, A.J., O'Donnell, L.J., 2020. SlicerDMRI: Diffusion MRI and Tractography Research Software for Brain Cancer Surgery Planning and Visualization. *JCO Clin Cancer Inform* 4, 299–309.
- Zhang, F., Savadjiev, P., Cai, W., Song, Y., Rathi, Y., Tunç, B., Parker, D., Kapur, T., Schultz, R.T., Makris, N., Verma, R., O'Donnell, L.J., 2018a. Whole brain white matter connectivity analysis using machine learning: An application to autism. *Neuroimage* 172, 826–837.
- Zhang, F., Wu, W., Ning, L., McAnulty, G., Waber, D., Gagoski, B., Sarill, K., Hamoda, H.M., Song, Y., Cai, W., Rathi, Y., O'Donnell, L.J., 2018b. Suprathreshold fiber cluster statistics: Leveraging white matter

- geometry to enhance tractography statistical analysis. *Neuroimage* 171, 341–354.
- Zhang, F., Wu, Y., Norton, I., Rathi, Y., Golby, A.J., O'Donnell, L.J., 2019. Test-retest reproducibility of white matter parcellation using diffusion MRI tractography fiber clustering. *Hum. Brain Mapp.* 40, 3041–3057.
- Zhang, F., Wu, Y., Norton, I., Rigolo, L., Rathi, Y., Makris, N., O'Donnell, L.J., 2018c. An anatomically curated fiber clustering white matter atlas for consistent white matter tract parcellation across the lifespan. *Neuroimage* 179, 429–447.
- Zhang, F., Xue, T., Cai, W., Rathi, Y., Westin, C.-F., O'Donnell, L.J., 2022c. TractoFormer: A Novel Fiber-Level Whole Brain Tractography Analysis Framework Using Spectral Embedding and Vision Transformers, in: *Medical Image Computing and Computer Assisted Intervention – MICCAI 2022*. Springer Nature Switzerland, pp. 196–206.
- Zhang, N., Nex, F., Vosselman, G., Kerle, N., 2023. Lite-mono: A lightweight CNN and transformer architecture for self-supervised monocular depth estimation, in: *2023 IEEE/CVF Conference on Computer Vision and Pattern Recognition (CVPR)*. Presented at the 2023 IEEE/CVF Conference on Computer Vision and Pattern Recognition (CVPR), IEEE, pp. 18537–18546.
- Zheng, Y., Gindra, R.H., Green, E.J., Burks, E.J., Betke, M., Beane, J.E., Kolachalama, V.B., 2022. A Graph-Transformer for Whole Slide Image Classification. *IEEE Trans. Med. Imaging* 41, 3003–3015.